DLR-IB-AS-BS-2022-70

On allowable surface tolerances for laminar flow

Geza Schrauf

Deutsches Zentrum für Luft- und Raumfahrt e.V.
Institut für Aerodynamik und Strömungstechnik
Braunschweig

Deutsches Zentrum
DLR für Luft- und Raumfahrt

Bericht des Instituts für Aerodynamik und Strömungstechnik
Report of the Institute of Aerodynamics and Flow Technology

DLR-IB-AS-BS-2022-70

Geza Schrauf

Herausgeber:
Deutsches Zentrum für Luft- und Raumfahrt e.V.
Institut für Aerodynamik und Strömungstechnik
Lilienthalplatz 7, 38108 Braunschweig

ISSN 1614-7790

Stufe der Zugänglichkeit: 1
Braunschweig, im Juni 2022

Institutsdirektor:
Prof. Dr.-Ing. habil. C.-C. Rossow

Verfasser:
Dr. rer. nat. Geza Schrauf

Abteilung: Transportflugzeuge
Abteilungsleiter:
Dr.-Ing. H. Freiherr Geyr von Schweppenburg

Der Bericht enthält:
24 Seiten
17 Bilder
2 Tabellen
21 Literaturstellen

Inhaltsverzeichnis

1. Introduction

The surface of a metallic or painted wing is not mathematically smooth, but has a certain roughness. In addition, air flows are influenced by certain unavoidable design and manufacturing irregularities. These different sources of roughness are referred to in various terms.

Overall surface roughness is distributed over the entire surface. Therefore, it is called “distributed roughness.” It is often compared to the roughness of sandpaper so that we also encounter the terms “sandpaper roughness” or “sand roughness.”

Forward and backward steps, as well as gaps, are the sources of irregularities unavoidably resulting from design. The wing of a transport aircraft consists of a load-carrying center part, the wing-box[1], as well as leading and trailing edge parts which are attached to wing box at front and rear spar. At this attachment, forward and backward steps and gaps often occur, often parallel to the front spar, i.e. across the line of flight. Their effect on transition is generally studied in two-dimensional boundary layer flow.

Other sources of irregularity are those that are built in during the manufacturing process. The leading edge is attached with the help of bolts and rivets. The heads of these are sometimes not completely flush with the surface. Wherever a bolt or rivet head is above the surface it will influence the airflow as a three-dimensional disturbance. These disturbances are modelled archetypally as small cylinders attached to the surface. They have been investigated in various wind tunnel and flight experiments.

All of the above-mentioned surface irregularities can be detrimental to laminar flow. To avoid early transition, we have to define limits for allowable disturbances as a guideline for design and manufacturing. Our task is to make this definition such that it is “good enough” rather than ideal, for if we are too strict on surface quality requirements, we would make design and manufacturing of laminar surfaces so expensive that laminar implementation would become economically unfeasible. The definition of appropriate surface requirements — not too strict, not too loose — is thus central for the practical application of laminar flow, whether natural laminar flow (NLF) or hybrid laminar flow (HLFC).

[1] The wing box often contains the fuel tank. Therefore, we apply laminar flow control (LFC) by suction only at the leading edge before the front spar and use natural laminar flow, i.e. a suitable shape of the wing box, to delay the laminar-turbulent transition behind the front spar. This combination is called hybrid laminar flow control (HLFC).

2. Input data and required surface quality criteria

The surface quality requirements will be set up for the lowest flight altitude and the highest Mach number for which the HLFC system should operate, because this is the most critical case. Flying with a lower Mach number and (or) at higher altitude will result in a thicker boundary layer for which the requirements become less strict.

For this study, we considered the case with **flight altitude 33000 ft, Mach 0.85, CL = 0.5**.

For this flight case, we received boundary layer input data in the BLI-format for nine spanwise sections. The data was carefully checked, slightly corrected, and renamed with our naming convention. The cases are presented in Table 1:

BL-Sections		Y	Y/Semi-Span	CASE
#	Name	[mm]	[-]	
0	S37	10612	0,368	H33M85CL50S37U
1	S44	12744	0,443	H33M85CL50S44U
2	S52	14876	0,517	H33M85CL50S52U
3	S59	17012	0,591	H33M85CL50S59U
4	S66	19147	0,665	H33M85CL50S66U
5	S74	21243	0,738	H33M85CL50S74U
6	S81	23338	0,810	H33M85CL50S81U
7	S89	25491	0,885	H33M85CL50S89U
8	S96	27644	0,960	H33M85CL50S96U

Table 1: Input data.

In Figure 1, we present the two inboard sections S37 and S44, the middle section S66, as well as the outer section S96. It can be seen that the wing surface at the leading is three-dimensional, i.e. it cannot be developed into a plane.

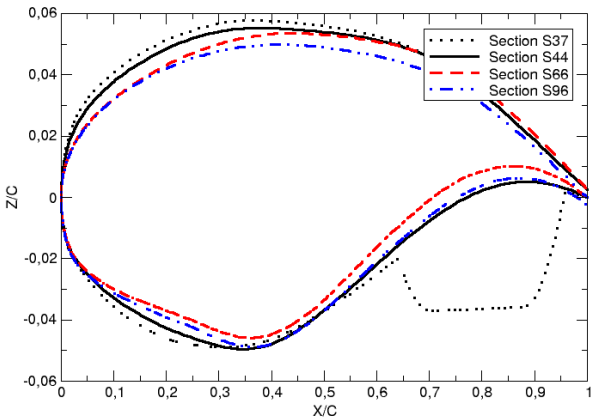

Figure 1: Comparison of several wing sections.

The input data contains non-zero suction up to 19% chord, i.e. the suction panel will probably extend up to around 20%, where it has to be connected to the surface of the wing box. At this location we expect steps or gaps parallel to the front spar which has a local sweep angle of around 30°: This has to be taken into consideration. Furthermore, if we have used bolts and rivets for the attachment, we also need the criteria for three-dimensional roughness elements. Because, in preliminary design, the details of the attachment of the HLFC leading edge to the wing box are not yet defined, we assume that the steps, gaps, and rivet heads occur in the region between 15% and 30% chord.

Furthermore, we need to make sure that the painted surface of the wing box is smooth enough not to cause early transition by distributed roughness. We assume that transition will occur before 60% chord, so that the criterion for distributed roughness should be satisfied behind the suction panel up this location (It does not make sense to consider distributed surface roughness over the micro-perforated suction panel).

For our project, we need the following surface quality criteria to continue with the structural design:

$0.15 < X/C < 0.30$	Criteria for forward- and backward facing steps, as well as gaps, and criteria for three-dimensional disturbances.

3. Two-dimensional imperfections

In early wind tunnel experiments, the influence of a circular, spanwise wire in a two-dimensional boundary layer along a flat plate was often investigated. The goal of these “trip wire” experiments was to provoke laminar-turbulent transition in the boundary layer of the wind-tunnel model to make the flow representative for the full-sized aircraft. A typical set-up of a study with a flat-plate boundary layer is shown in Figure 2.

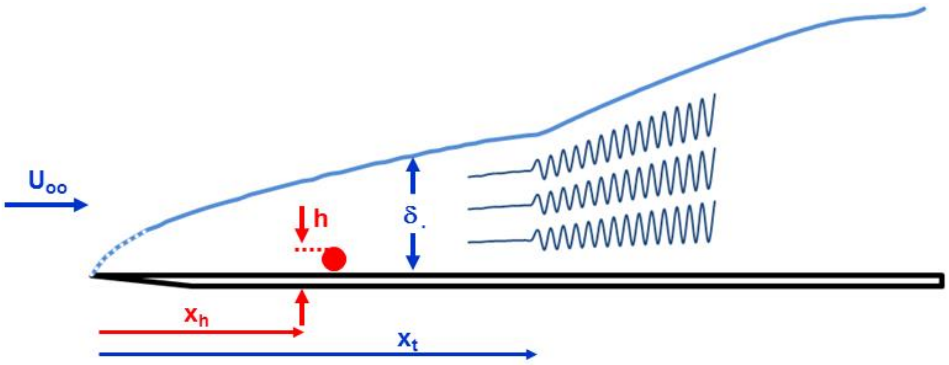

Figure 2: Circular, spanwise wire in a flat-plate boundary layer.

The wire is located at the distance X_h from the leading edge and has a diameter h, which is the height of the disturbance. Laminar-turbulent transition in the boundary layer occurs at the distance X_t from the leading edge. We can now vary the velocity U_∞ of the oncoming flow as well as the position and the diameter (but not the shape) of the wire. The transition location X_t depends on the quantities, U_∞, X_h, h, as well as on the kinematic viscosity $\nu = \mu/\rho$ of the air. In total we have the five quantities $X_t, X_h, h, U_\infty, \nu$, which depend on the two basic dimensions length and time. According to the Buckingham π Theorem, the problem can be described with only three non-dimensional quantities [1]. We use:

- a non-dimensional roughness height,
- a non-dimensional roughness location, and
- a Reynolds number.

Regarding the Reynolds number, the following five are often used in conjunction with roughness effects:

$$Re_t = \frac{U_\infty x_t}{\nu}$$

$$Re_h = \frac{U_e h}{\nu} \quad \text{extension of} \quad Re_h = \frac{U_\infty h}{\nu}$$

$$Re_{hh} = \frac{U_h h}{\nu} \quad \text{Schiller (1932): rough pipes}$$

$$Re_{\tau h} = \frac{U_\tau h}{\nu} \quad \text{with} \quad U_\tau = \sqrt{\tau_w/\rho}$$

$$Re_{\delta_{1,i}} = \frac{U \delta_{1,i}}{\nu} \quad \text{with } U \text{ at } x_h \text{ or } x_t$$

The second Reynolds number Re_h is an extension of the originally proposed one, computed with the velocity U_∞ of the oncoming free-stream instead of the boundary-layer edge-velocity U_e at the location x_h of the roughness element. The velocity U_e is obtained for the boundary layer along the surface WITHOUT the roughness.
The velocity U_h in the definition of the third Reynolds number Re_{hh} is the velocity at the normal distance h from the surface measured at the location of the roughness element, again in the flow WITHOUT the roughness element. This Reynolds number was introduced by L. Schiller [2], when he investigated the influence of surface roughness in pipes. The fourth Reynolds number is computed with the wall shear rate.
Regarding 2D imperfections, we assume that a 2D roughness mainly affects the amplification of Tollmien-Schlichting waves and has only a weak influence on the amplification induced by cross-flow vortices [3].

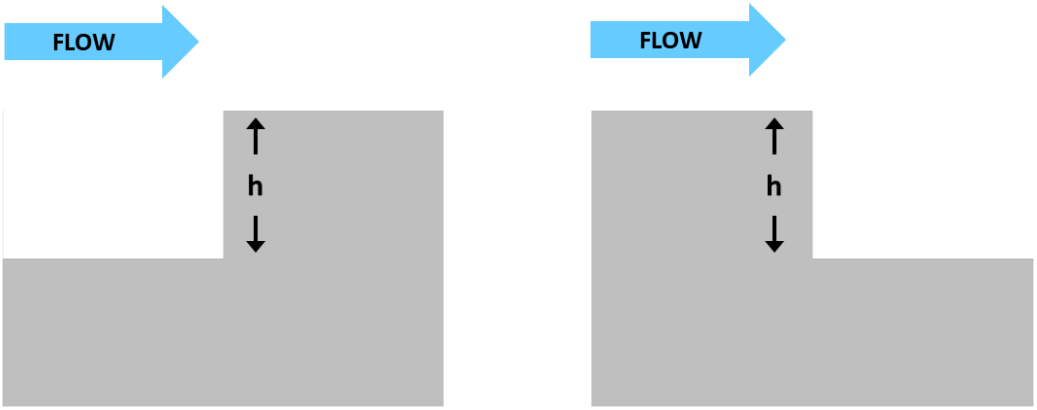

Figure 3: Sketch of a forward and a backward facing step.

3.1. Forward snd backward facing steps

3.1.1. Steps across line of flight

3.1.1.1. Classical criteria

The classical criteria for forward and backward facing steps, proposed by Nenni&Gluyas [4], are:

(C1mod) Backward facing step $$Re_h = \frac{U_e\, h}{\nu} < 900$$

(C2mod) Forward facing step $$Re_h = \frac{U_e\, h}{\nu} < 1800$$

These classical criteria can be used to obtain a first estimate of the allowable step heights.

Figure 4: The X21 research aircraft.

The original Nenni&Glyas criteria depend only on the velocity at the edge of the boundary layer. However, it is known that the [in]stability of the boundary layer in the neighborhood of the step, as well as behind it, plays an important role [5]. In order to include the stability properties of the boundary layer, so-called variable N-factor methods were introduced [6, 7, 8, 9]. Because these methods are not yet calibrated for general application, we do not apply them in this report. However, an application of [8,9] by ONERA would be welcomed.
For the design of the BLADE flight test demonstrator [10], forward and backward facing steps were investigated at flight Mach and Reynolds numbers in the cryogenic Rohr wind tunnel (KRG) [11] and also in the European Transonic Wind Tunnel [12]. These tests confirmed that the boundary layer thickness and the pressure gradient in the neighborhood of the step are important parameters which should be taken into account. Unfortunately, we were not able to condense the new information into practical criteria for general application.
However, one outcome was that, in the range 0.15 < X/C <0.30, the criterion C2mod can be relaxed to

(C2mod2)
$$Re_h = \frac{U_e h}{\nu} < 3600 - 4500.$$

Laminarity was unaffected with $Re_h = 3600$, but not in all cases with $Re_h = 4500$. For X/C > 0.3, an upper value of 4500 was possible. However, this value should be used with great care.

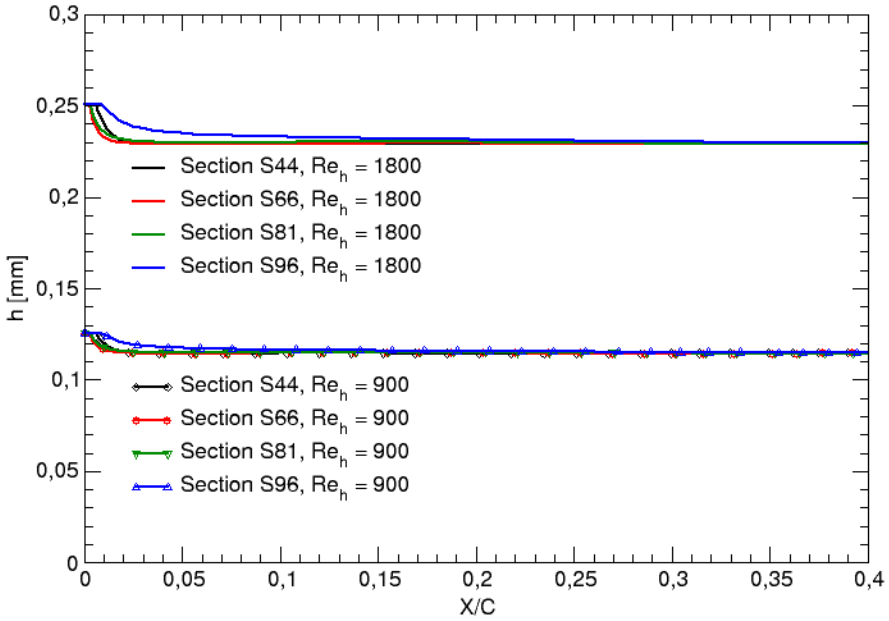

Figure 5: Roughness heights obtained with $Re_h = 900$ and $Re_h = 1800$.

3.1.1.2. Application of classical criteria

In Figure 5 we present the h-values of the function

$$h = Re_h \frac{\nu}{U_e},$$

obtained for $Re_h = 900$ and $Re_h = 1800$ for the four sections S44. S66, S81, S96. At the attachment line, the boundary-layer edge velocity U_e becomes smaller, making h become larger. Because this is physically unlikely, we limit h with the classical Nenni-Gluyas criterion

$$h = Re_h \frac{\nu}{U_\infty},$$

i.e. we apply the modified Nenni-Gluyas criteria in the form

$$h = Re_h \, min\left\{\frac{\nu}{U_\infty}, \frac{\nu}{U_e}\right\}.$$

With $Re_h = 900$, we obtain for 0.1 < X/C < 0.4 the value $h \approx 0.12\ mm$ for a backward-facing step, which is in line with our previous value $h \approx 0.13\ mm$ estimated for the higher design altitude of 36000 ft [13].

The computed value for $Re_h = 1800$ is $h \approx 0.23\ mm$, which again fits to our previous value of value $h \approx 0.26\ mm$ for the higher flight altitude given in [13]. However, our experience is that, for a forward-facing step, the C2mod-value can be relaxed by a factor of 2 or 2.5, i.e. to $0.46\ mm - 0.57\ mm$. Therefore, we allow in the region 0.15 < X/C < 0.30 a forward-facing step with a maximal height of $h \approx 0.50\ mm$.

These values for a backward or a forward-facing step are also valid for multiple steps if they are far enough apart, for example, more than 10% chord. It is common practice to halve the allowable step sizes for multiple steps closely following each other.

3.1.1.3. A comment on a proposed joint concept

One of the proposed concepts for the joint between the HLFC leading edge and the wing box is shown in Figure 6. With this concept, the titanium of the leading edge would simply end on a small ramp

Figure 6: Proposed joint concept.

and form a backward-facing step. The thickness of the titanium sheet is 0.8 mm. Thus, the height of this step would be more than six times larger than the limit value $h \approx 0.12\ mm$, resulting in a loss of laminarity. We know from previous wind tunnel tests that the criterion $Re_h = 900$ for backward-facing steps is strict and cannot be relaxed. This means that the end of the titanium sheet would have to be thinned to 0.1 mm.

3.1.2. Steps in line of flight

The boundary layer is very sensitive with respect to steps in line of flight. Therefore, such steps should be avoided. If this is not possible, then a turbulent wedge will be unavoidable.

Any high-lift system will use slats or Kruger flaps. For laminarity, it would be best to have one large element extending over the whole span. However, regarding systems and maintenance aspects, several smaller elements are preferable. Therefore, we have to find a compromise: This, could be found in the maximal spanwise extension, which would allow an airport maintenance crew to exchange a damaged element.

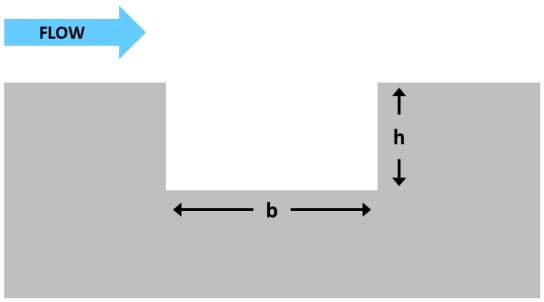

Figure: 7: Sketch of a gap.

3.2. Gaps

3.2.1. Gaps across line oif flight

The classical Nenni&Gluyas [4] criterion for a gap is

$$Re_b = \frac{U_\infty b}{\nu} = 15000,$$

where b is the width of the gap. As before, we replace the free-stream velocity U_∞ with the velocity U_e at the edge of the boundary layer. The allowable gap width is then obtained as

$$b = \frac{\nu}{U_e} 15000.$$

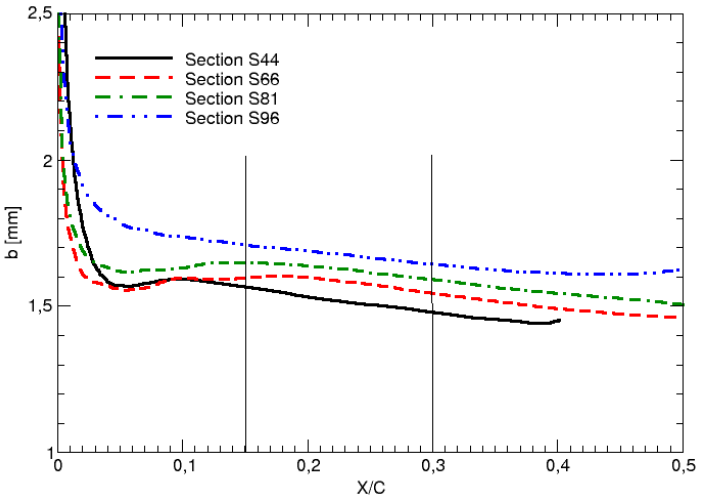

Figure: 8: Allowable gap widths for several sections.

Applying the formula for the region $0.15 \leq X/C \leq 0.3$, we obtain the following values:

	X/C = 0.15	X/C = 0.23
Section	b [mm]	b [mm]
S44	1,56	1,48
S66	1,59	1,54
S81	1,64	1,59
S96	1,70	1,64

In contrast to steps, the author has less experience with the influence of gaps on laminar-turbulent boundary transitions. Some experimental observations indicate that some secondary flow might be induced in a gap when it is not perpendicular to the flow. The flow in the gap might have local outflows which would trigger turbulence.

Therefore, we recommend a maximal allowable gap width of 1 mm. To avoid a flow within the gap, we recommend that the gap be closed with some filler material. This filler material has to be able to withstand the large temperature variation from +80 C (on ground in the sun) to -80°C (the standard temperature at 36000 ft is -56°C). The expansion and shrinking of the material due to the temperature variations has to be taken into account.

3.2.2. Gaps in line of flight

Gaps may be unavoidable at structural interfaces. However, gaps in line of flight should be avoided. This has to be taken into account by the structural design.

4. Three dimensional imperfections

4.1. Set-up of a criterion

Rivet and bolt heads, and insect debris form small, local surface disturbances. If large enough, these can cause a turbulent wedge. The typical 3D-disturbance investigated in wind tunnel tests and flight experiments is a small upright cylinder attached to the surface. A sketch of the flow pattern generated by such an element, taken from [14], is shown in Figure 9.

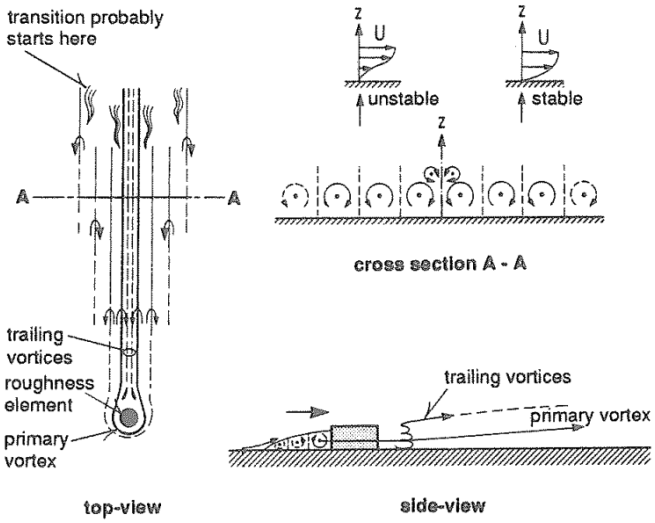

Figure 9: Schematic sketch of the vortex system behind a 3D-disturbance.

We see that the disturbance creates a system of streamwise vortices which either decays or leads to a turbulent wedge which is generated by secondary instabilities.
In the classic literature [15, 16, 17], we find engineering criteria based on the Reynolds number

$$Re_{hh} = \frac{u_h h}{\nu}.$$

The criteria are:

$$\text{Klebanoff et al.:} \quad Re_{hh} = 500 - 800,$$

$$\text{Gregory et al.:} \quad Re_{hh} = 440,$$

$$\text{Tani:} \quad Re_{hh} = 600 - 800.$$

In [18], Doenhoff&Brasloff compiled many experimental results. They plot $\sqrt{Re_{hh}}$ over the geometric shape parameter D/h of the disturbance, D being its diameter and h its height (c.f. Figure 10).

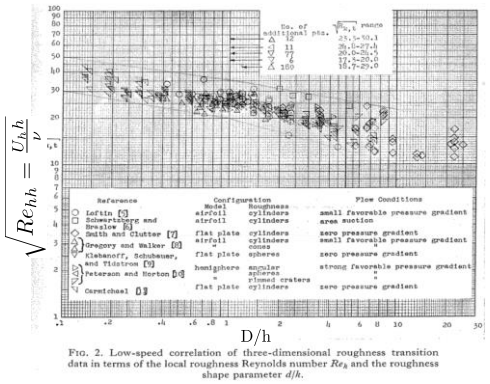

FIG. 2. Low-speed correlation of three-dimensional roughness transition data in terms of the local roughness Reynolds number Re_k and the roughness shape parameter d/k.

Figure 10: Collection of experimental results as of 1962.

Within the EC-project RECEPT [19, 20], direct numerical simulations (DNS) were performed. The calculations confirmed that Re_{hh} is indeed a useful quantity to account for 3D-excrescences. Furthermore, the calculations show a difference in the vortex system behind the disturbance between two- and three-dimensional flow. In two-dimensional flow, the vortices on both sides of the disturbance are of equal strength as shown in Figure 11.

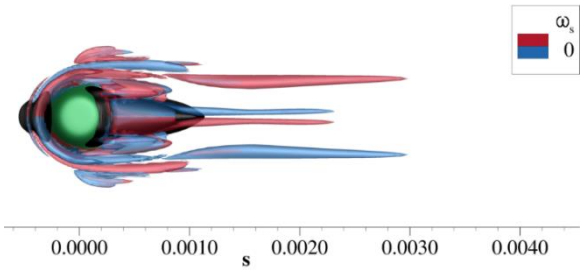

Figure 11: Two dominant counter-rotation vortices with equal strength in 2D-flow.

A three-dimensional boundary layer, such as the one on a swept wing, has an intrinsic rotation caused by the cross-flow velocity profiles which have an inflection point. This intrinsic rotation strengthens the vortex with the same rotation and weakens the other one as seen in Figure 12.

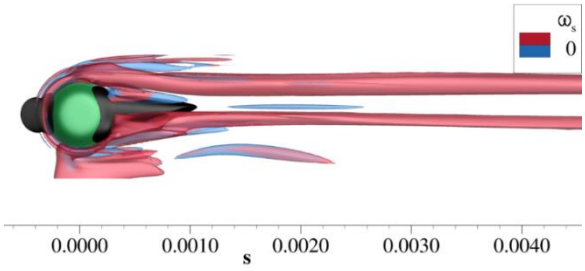

Figure 12: In 3D-flow, the two dominant counter-rotation vortices have different strengths.

If the Reynolds number is increased, secondary instabilities will appear, as can be seen in Figure 13. A further increase to $Re_{hh} = 564$ will definitively cause turbulence (cf. Figure 14).

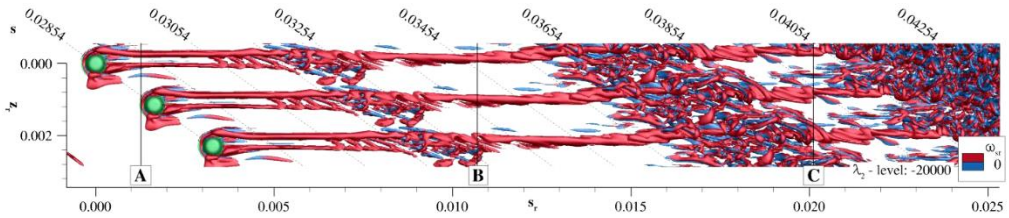

Figure 13: Secondary instabilities for $Re_{hh} = 487$.

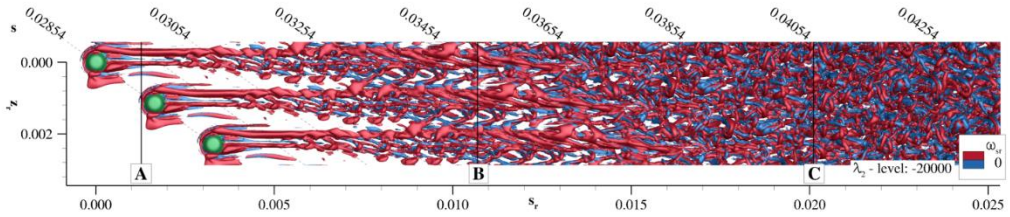

Figure 14: Flow break-down to turbulence for $Re_{hh} = 564$.

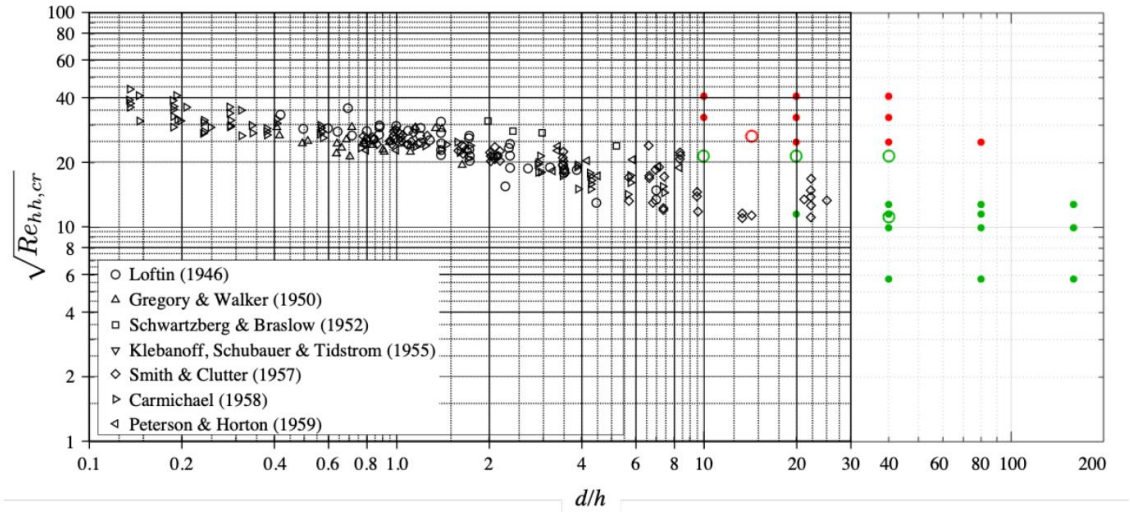

Figure 15: RECEPT results included in Fig. 10.

Wind tunnel tests with 3D roughness elements were performed within RECEPT. In Figure 15, Örlü et al. [21] included the new experimental results in the Doenhoff&Branslow Figure 10. Red and green dots correspond to cases where flow in the flow remained laminar or transitioned to turbulent, respectively. We see that the Re_{hh}-values of the new results are in line with the classical ones.

Taking into account these new results, we propose the following criterion for 3D-disturbances:

$$Re_{hh} < 200\ (-300) \quad \text{no influence,}$$

$$Re_{hh} = 400 - 500 \quad \text{beginning of transition,}$$

$$Re_{hh} > 550 \quad \text{transition to turbulence.}$$

4.2. Application of the criterion

In order to propose limits for allowable three-dimensional disturbances, we compute the height h for several prescribed values of the Reynolds number Re_{hh}. In Figure 16, we present a comparison of the heights obtained with $Re_{hh} = 400$ for the sections S44, S66, S81, S96. All heights are of the same magnitude, however, the smallest values occur for the outer section S96. Therefore, we consider this section for the determination of the allowances. In Figure 17 we plot the h-values obtained with the four different Reynolds numbers $Re_{hh} = 200, 400, 500, 800$ over X/C.

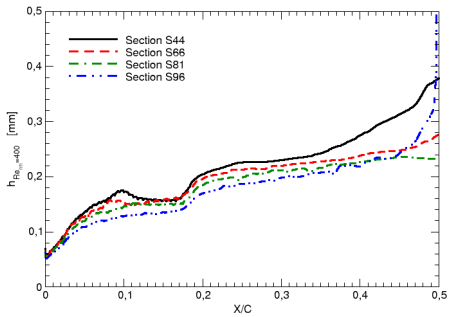

Figure 16: Heights computed with $Re_{hh} = 400$ for sections S44, S66, S81, S96.

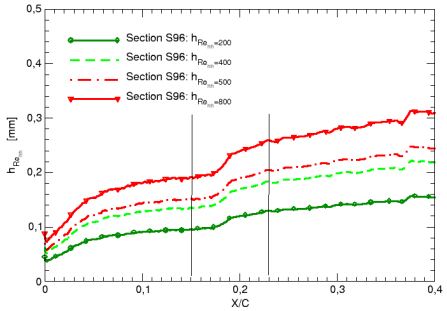

Figure 17: Heights obtained with different Re_{hh} for section S96.

At $X/C = 0.15$ and 0.23 we obtain the following values:

X/C = 0.15		X/C = 0.23	
Re_{hh}	h [mm]	Re_{hh}	h [mm]
200	0,09	200	0,13
400	0,13	400	0,18
500	0,15	500	0,20
800	0,19	800	0,26

Table 2: h-values for different Reynolds numbers Re_{hh} at two chordwise locations.

The h-values obtained with $Re_{hh} = 200$ are conservative and the ones with $Re_{hh} = 400$ are close to the limit. In view of this, we propose the following allowable heights for 3D disturbances:

0.15 < X/C < 0.23	0.11 mm
0.23 < X/C	0.16 mm

5. Conclusions

In this report we present an overview on the classical criteria for forward and backward facing steps, gaps, as well as criteria for three dimensional disturbances. These criteria are generally important for laminar wing design, but especially for the design of the attachment of an HLFC leading edge to the front spar. Each design concept must comply with the allowables, in order to avoid transition at the joint.

For the upper side of the wing, we found the following allowable heights for the investigated surface imperfections:

Backward facing steps:	0.15 < X/C < 0.30	Step height < 0.12 mm	
Forward facing steps:	0.15 < X/C < 0.30	Step height < 0.50 mm	
Gaps:	0.15 < X/C < 0.30	Gap width < 1 mm	(gaps should be filled)
3D-Disturbances.	0.15 < X/C < 0.23	Height < 0.11 mm	
	0.23 < X/C	Height < 0.16 mm	

6. Literature

[1] H. L. Dryden: “Review of Published Data on the Effect of Roughness on Transition from Laminar to Turbulent Flow.” Journal of the Aeronautical Sciences, Vol. 20, 1953, pp. 477-482.

[2] L. Schiller:“Die Strömung in rauhen Rohren.“ In: L. Schiller (Ed.) "Handbuch der Experimental-physik." Band 4 "Hydro- und Aerodynamik," 4. Teil "Rohre, offene Gerinne, Zähigkeit." Akad. Verlagsgesellschaft m.b.H. (Leipzig), 1932.

[3] G. Schrauf: “Influence of surface imperfections (surface roughness, steps, gaps, ...) and suction on transition.” ERCOFTAG Course on Transition Modelling, 21-22 May 2015, GE Global Research Center, Munich, Germany.

[4] J. P. Nenni, G. L. Gluyas: “Aerodynamic Design and Analysis of an LFC Surface.” Astronautics and Aeronautics, July 1966, pp 52 - 57.

[5] G. Schrauf: “On Allowable Step Heights: Lessons Learned from the F100 and ATTAS Flight Tests.” ECCOMAS, 11-15 June 2018, Glasgow, UK. https://elib.dlr.de/124546/.

[6] J.D. Crouch, L.L. Ng: “Variable N-Factor Method for Transition Prediction in Three-Dimensional Boundary Layers.” AIAA-Journal Vol. 38, No. 2, February 2000, pp. 211-216.

[7] J.D. Crouch, V.S. Kosorygin, L.L. Ng: “Modelling the effects of steps on boundary-layer transition.” In: R. Govindarajan (ed.), Sixth IUTAM Symposium on Laminar-Turbulent Transition, 2006, Springer, pp 37-44.

[8] J. Perraud, A. Séraudie: “Effects of steps and gaps on 2D and 3D transition,” ECCOMAS 2000.

[9] J. Perraud, D. Arnal, A. Séraudie, D. Tran: “Laminar-turbulent transition on aerodynamic surfaces with imperfections,” RTO AVT-111 Symposium, Prague, 4-7 October 2004.

[10] Breakthrough Laminar Aircraft Demonstrator in Europe (BLADE) https://en.wikipedia.org/wiki/Breakthrough_Laminar_Aircraft_Demonstrator_in_Europe#Development.

[11] Kryo-Rohrwindkanal Göttingen, https://www.dnw.aero/wind-tunnels/krg/.

[12] European Transonic Wind Tunnel, https://www.etw.de/.

[13] G. Schrauf: “Some Remarks on Surface Quality for the LPA 1.4.4 HLFC Wing.” DLR-Presentation 25.02.2019.

[14] A.C. de Bruin: “Experiments and theoretical considerations regarding the allowable surface roughness height in laminar flow.” First European Forum on Laminar Flow Technology, Hamburg, Germany, March 16-18, 1992.

[15] P.S. Klebanoff, G.B. Schubauer, K.D. Tidstrom: “Measurements of the Effect of Two-Dimensional and Three-Dimensional Roughness Elements on Boundary-Layer Transition.” Journal of the Aeronautical Sciences, Vol. 22, 1955, pp. 803-804.

[16] N. Gregory, W.S. Walker: “Part I: The effect on Transition of Isolated Surface Excrescences in the Boundary Layer.” A.R.C., R&M No. 2779, 1956.

[17] I. Tani: “Effect of Two-Dimensional and Isolated Roughness on Laminar Flow.” In: G. V. Lachmann (Ed.), Boundary Layer and Flow Control, Vol. 2, Pergamon Press, 1961.

[18] A. E. Doenhoff, A. L. Braslow: “The Effect of Distributed Surface Roughness on Laminar Flow.” In: G. V. Lachmann (Ed.), Boundary Layer and Flow Control, Vol. 2, Pergamon Press, 1961.
[19] H. Kurz, M. J. Kloker: “Direct Numerical Simulations of Roughness Elements in a 3-d Boundary Layer.” RECEPT Final Meeting, 28-29 April 2015, Stockholm.
[20] H. Kurz, M. J. Kloker "Receptivity of a swept-wing boundary layer to micron-sized discrete roughness elements." JFM Vol. 755, 2014, 62-82.
[21] R. Örlü, N. Tillmark P. H. Alfredsson: "Measured critical size of roughness element.” Technical Report TR D1.14. RECEPT Project, 2015.

DLR-IB-AS-BS-2022-70

Geza Schrauf

Verteiler:

Institutsbibliothek AS	1 Exemplar
Verfasser	1 Exemplar
Institutsleitung	1 Exemplar
Abteilungsleiter	1 Exemplar
Deutsche Bibliothek in Frankfurt/Main	2 Exemplare
Niedersächsische Landesbibliothek Hannover	1 Exemplar
Techn. Informationsbibliothek Hannover	1 Exemplar
Zentralbibliothek BS	1 Exemplare
Zentralarchiv GÖ	1 Exemplar